Second axial Fe^{3+} center in stoichiometric lithium tantalate

G. Malovichko[a] and R. Petersen
Physics Department, Montana State University, Bozeman, Montana 59717

Ch. Bäuman
Department of Physics, University of Osnabrück, Osnabrück 49074, Germany

V. Grachev[b]
Physics Department, Montana State University, Bozeman, Montana 59717

(Received 21 December 2005; accepted 22 April 2006; published online 31 July 2006)

The axial Fe^{3+} center Fe1 with the crystal field parameter $b_2^0 \approx 3130 \times 10^{-4}$ cm^{-1} is well studied in congruent lithium tantalate crystals. The second axial Fe^{3+} center Fe2 was discovered and investigated by the electron paramagnetic resonance in stoichiometric samples prepared by vapor transport equilibrium treatment. The crystal field parameter of the Fe2 center ($b_2^0 \approx 2050 \times 10^{-4}$ cm^{-1}) is significantly smaller than for Fe1. The electron nuclear double resonance measurements have shown that hyperfine interactions of the Fe^{3+} electrons with the surrounding Li nuclei for Fe2 are stronger than for Fe1. Therefore, the conclusion was made that in the case of Fe2 center the iron ion substitutes for Ta and has Li nuclei in the nearest neighborhood, whereas in the case of Fe1 center it substitutes for Li, has Ta nuclei as nearest neighbors and Li nuclei in the second shell only. © *2006 American Institute of Physics*. [DOI: 10.1063/1.2215349]

I. INTRODUCTION

The determination of structures of centers created in lithium tantalate (LT) ($LiTaO_3$) by impurity ions, including those of transition metals and rare-earth elements, is one of the most important tasks in defect study of this material. The elucidation of the position of these impurities in the lattice, their nearest surroundings, and charge compensators is vital for both fundamental science and tailoring properties of this material for various applications. It is known that iron ions play important role in the photorefractive effect and holographic storage.[1–4] Because of this reason Fe are intensively investigated in LT crystals.[5,6] Spectroscopic parameters of the main axial Fe^{3+} center, called Fe1 in the following, were obtained long ago:[7] $g \approx 2.00$ and $b_2^0 = 3300 \times 10^{-4}$ cm^{-1}. Recently, the parameters were determined more accurately.[8,9]

At room temperatures the LT lattice has $R3c$ space symmetry having the same axial C_3 point symmetry for three sites: the Li and Ta sites and the structural vacancy. It creates difficulties for the determination of impurity ion locations, since many techniques including the electron paramagnetic resonance (EPR) and optical methods cannot distinguish these positions. The electron nuclear double resonance[7] (ENDOR) study has shown that Fe^{3+} substitutes for Li^+, accompanied by some local disorder among the neighbors of this site, most probably an unknown defect being present in the first Li sphere.

Similar to isostructural lithium niobate (LN) crystals, high quality optical LT crystals are usually grown from congruent melt with the essential lithium deficit: about 6% in LN and 1.6% in LT. Therefore, these crystals contain a high concentration of intrinsic defects, which can serve as charge compensators for nonisovalent substituting or interstitial impurities. Crystals with essentially reduced concentration of intrinsic defects (stoichiometric or nearly stoichiometric) have properties, which differ from properties of conventional congruent samples. Sometimes the difference is one or two orders of magnitude.[10] It gives an opportunity to improve crystals adjusting them for various applications. Three basic procedures developed initially for obtaining stoichiometric LN crystals—postgrowth vapor transport equilibrium (VTE) treatment of congruent samples in Li-rich powder,[11,12] double crucible growth,[13,14] and growth from the melt with addition of potassium[15–19]—are now successfully applied to LT.[20–25] Lack of intrinsic defects in stoichiometric samples often causes a change of the charge compensation mechanisms and appearance of additional paramagnetic centers.[26–28]

Here we report about the EPR/ENDOR study of the Fe^{3+} centers in stoichiometric LT.

II. EXPERIMENT

Stoichiometric LT (sLT) samples were obtained with the help of VTE treatment of congruent LT (cLT) samples. Details of the procedure and characterization of the samples are described in Ref. 29. The EPR/ENDOR spectra were measured using our Bruker Elexsys 560 spectrometer at 9.8 (X band) and 34.4 (Q band) GHz. Several samples with concentrations of iron from 0.01 to 0.08 wt % in the melt (which correspond to 1.1×10^{19} and 6.7×10^{19} cm^{-3} in the crystals[29]) were studied.

Low intensity EPR signals of trace impurities Fe^{3+} and Cu^{2+} were registered in an undoped sLT sample. Simulation of the Fe^{3+} spectra has shown that the lines belong to Fe1 centers.

Comparison of the EPR spectra for congruent and sto-

[a]FAX: (406) 994 4452; electronic mail: malovichko@physics.montana.edu
[b]FAX: (406) 994 4452; electronic mail: grachev@physics.montana.edu

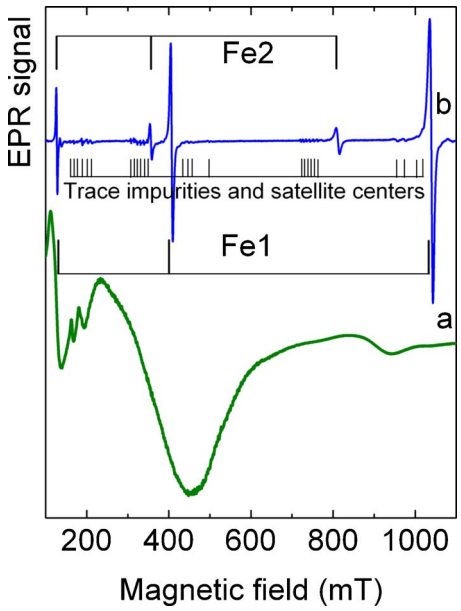

FIG. 1. (Color online) The EPR spectra of congruent (a) and stoichiometric (b) lithium tantalate doped with low concentration of iron. *X* band, room temperature, $\mathbf{B}\|\mathbf{x}$.

ichiometric crystals doped with relatively low concentration of iron (about 0.01 wt % in the melt) clearly demonstrates several important features that appeared in sLT (Fig. 1).

(a) All lines become significantly narrower.
(b) The lines acquire the symmetrical derivative shape of absorption signal.
(c) Many small lines of trace impurities and satellite centers become resolved.
(d) The second group of lines labeled Fe2 arises.

In this sample the relative intensities of the additional lines I_2 are several times smaller than the intensities of the lines attributed to the Fe1 center I_1. However, the lines of Fe1 and Fe2 have nearly equal intensities in sLT samples doped with 6.7×10^{19} cm^{-3} of Fe (Fig. 2).

The angular dependencies of the Fe1 and Fe2 centers were described by the spin Hamiltonian for electron spin $S=5/2$,

$$H=\beta\mathbf{B}\cdot\mathbf{g}\cdot\mathbf{S}+b_2^0O_2^0+b_4^0O_4^0+b_4^3O_4^3+c_4^3\Omega_4^3. \quad (1)$$

Here β is the Bohr magneton, $\mathbf{B}$ is the magnetic field, $\mathbf{g}$ is the g tensor, $\mathbf{S}$ is the spin, $O_2^0=O_2^0/3$, $O_4^q=O_4^q/60$, and $\Omega_4^q=\Omega_4^q/60$; O_k^q and Ω_k^q are the Stevens spin operators.

The LT unit cell has two molecules, which are transformed into each other by reflection in the glide mirror plane of the structure (**zy** plane). This means that each axial center, say *L*, has an electrically equivalent, but magnetically nonequivalent partner *R*. The spin-Hamiltonian parameters of both centers are equal with respect to their absolute values, but $b_4^3(L)=-b_4^3(R)$. The presence of two magnetically nonequivalent centers in the $R3c$ structures leads to a splitting of the EPR lines in **zx** plane when the magnetic field deviates from the **z** axis.[8,9,26]

Fitting of the observed angular dependencies (Figs. 3–5) was carried out with the help of VISUAL EPR program using

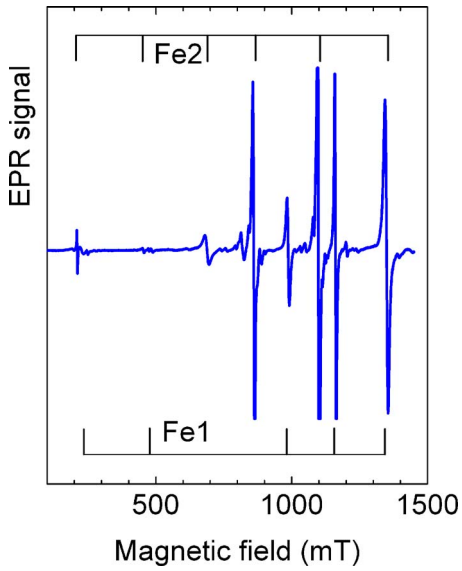

FIG. 2. (Color online) The EPR spectrum of sLT doped with 6.7×10^{19} cm^{-3} of Fe. *Q* band, room temperature, $\mathbf{B}\|\mathbf{x}$.

exact numerical diagonalization of the spin-Hamiltonian matrices. The parameters, which gave a value of about 3 mT for mean square root (MSR) deviation of the calculated resonance line positions from experimental ones, are collected in the Table I. For Fe1 centers the parameters cited in Refs 7–9 gave larger MSR deviation from experimental data measured in both *X* and *Q* bands.

The axial crystal field parameters for Fe1 and Fe2 have different temperature dependences: when the temperature decreases to 4 K the line splitting of Fe1 increases by 3.6%, whereas the line splitting of Fe2 center decreases by 1.1%.

Additional information about Fe2 centers was obtained with the help of ENDOR. The ENDOR measurements were performed in *Q* band at the lines in high magnetic fields. Using high magnetic fields increases distances between Larmor frequencies of Li, Ta, Fe, and other nuclei, and improves the line separation for different isotopes and nuclei. The measurements have shown that hyperfine interactions of iron electrons with surrounding lithium nuclei for Fe2 center are stronger than for Fe1 center (Fig. 6).

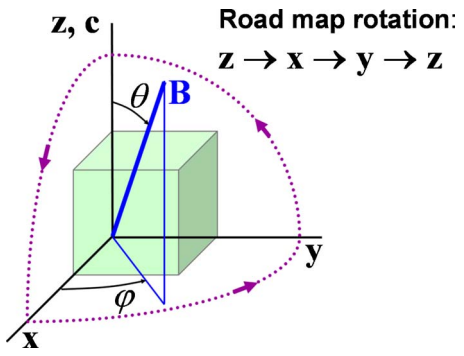

FIG. 3. (Color online) The road map angle runs from zero at $\mathbf{B}\|\mathbf{z}$ to 90° at $\mathbf{B}\|\mathbf{x}$, then from 90° at $\mathbf{B}\|\mathbf{x}$ to180° at $\mathbf{B}\|\mathbf{y}$, and from 180° at $\mathbf{B}\|\mathbf{y}$ to 270° at $\mathbf{B}\|\mathbf{z}$. It corresponds to the following changes of the θ and φ angles: $\theta=0°-90°$ at $\varphi=0°$, $\theta=90°$ at $\varphi=0°-90°$, and $\theta=0°-90°$ at $\varphi=90°$.

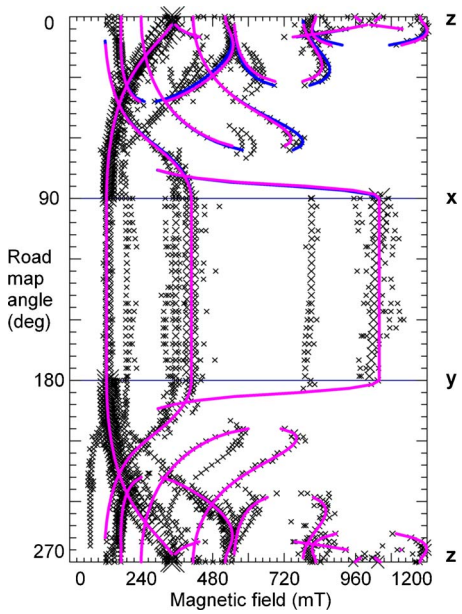

FIG. 4. (Color online) Angular dependencies (road map) of the EPR spectra of sLT doped with 6.7×10^{19} cm^{-3} of Fe. Symbols—experimental lines measured at helium temperatures in *X* band. Solid lines—best fit for the Fe2 centers with parameters indicated in Table I.

III. DISCUSSION

Since all details of the EPR spectra of the Fe2 lines (including angular dependencies of line positions and transition intensities) are completely described with the help of a spin Hamiltonian with spin $S=5/2$, we have to conclude the second centers are also Fe^{3+} ions. Both Fe1 and Fe2 centers have axial symmetry. The difference between characteristics of the Fe1 and Fe2 must be caused by the difference in the arrangement of ions around the Fe^{3+}. Most results of previous investigations of the Fe1 centers in cLT crystals confirm that in this case the Fe^{3+} ions substitute for Li^{+}. Cation vacancies always present in cLT serve as charge compensator of the excessive positive charge of Fe^{3+}_{Li}.

There are three reasonable hypotheses for an explanation of different surroundings for the Fe1 and Fe2 centers:

(1) Fe^{3+} occupy octahedral structural vacancy site,
(2) Fe^{3+} in Fe2 centers substitutes for Li^{+} but has additional defect on the center axis, and
(3) Fe^{3+} substitutes for Ta^{5+}.

An occupation of other positions in LT lattice or a presence of some defect out of the center axis does not agree with the observed axial symmetry of the Fe2 centers, and these possibilities must be discarded.

The first hypothesis cannot explain the observed relative changes of the Fe2 and Fe1 concentrations with the rise of total concentration of iron in the samples, since both vacancy site occupation and lithium substitution require similar charge compensators.

There are several arguments against the second hypoth-

TABLE I. Parameters of crystal field (in 10^{-4} cm^{-1}) and *g* tensor for Fe^{3+} center in $LiTaO_3$.

Center		Fe1			Fe2
$g_\perp$	1.995(2)	2.001(1)	2.000(2)	2.01(1)	2.012(10)
$g_\parallel$	1.995(2)	1.998(2)	2.012(3)	2.016(10)	2.02(1)
$\lvert b_2^0\rvert$	3300(30)	3200(7)	3075(7)	3132(20)	2050(20)
b_4^0		2±2	−60(10)	−54(20)	−80(20)
$\lvert b_4^3\rvert$		1393(10)	1200(200)	1300(200)	1300(300)
c_4^3			160(130)	0(300)	1300(300)
T (K)	15	305	300	300	300
Ref.	7	8	9	This work	This work

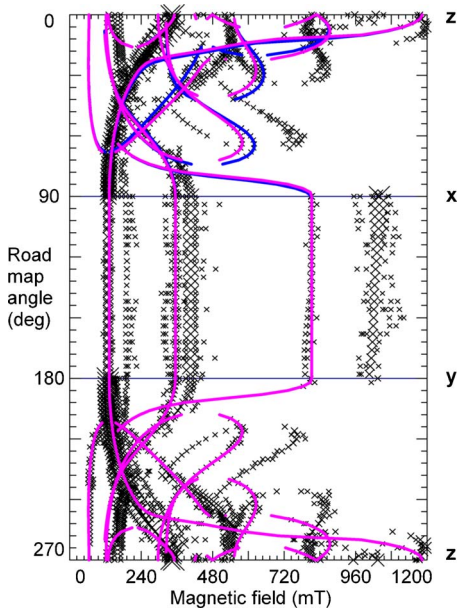

FIG. 5. (Color online) Angular dependencies (road map) of the EPR spectra of sLT doped with 6.7×10^{19} cm^{-3} of Fe. Symbols—experimental lines measured at helium temperatures in *X* band. Solid lines—best fitting for the Fe1 centers with parameters indicated in Table I. Fitting of lines for low-intensity satellite centers is not shown.

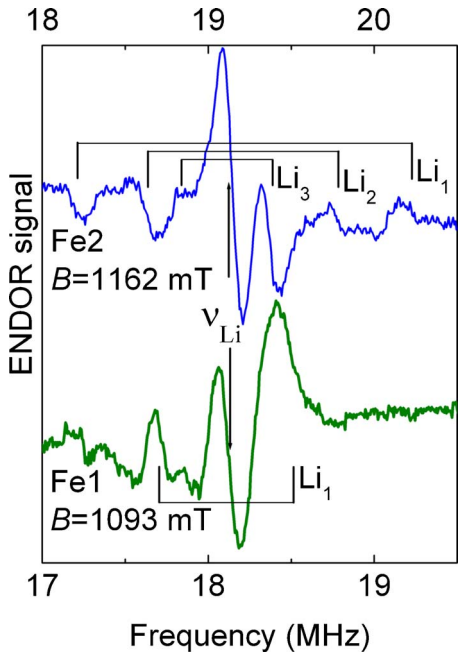

FIG. 6. (Color online) Fragments of the ENDOR spectra of Fe1 and Fe2 centers. *Q* band, $\mathbf{B}\|\mathbf{x}$, $T=5$ K. For a convenience of comparison the spectra are shifted to a common position of the Larmor frequency of Li nuclei.

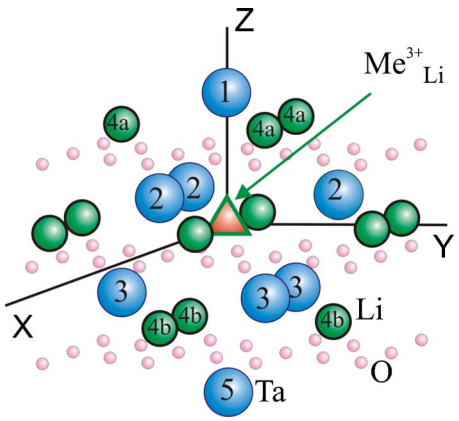

FIG. 7. (Color online) Schematic representation of surroundings of an ion substituting for Li in $LiTaO_3$.

esis. The Fe2 centers appear in sLT only. Would it be related to additional impurity defect in the nearest surrounding, it should exist in cLT too. This is not observed. Neutral complex such as $Fe^{3+}{}_{Li}$, interstitial O^{2-} could be created at the VTE treatment, and the charge compensation mechanism in this case is different from the Fe1 one. However, such complexes have usually significantly stronger axial crystal field.

The Fe^{3+} substitution for Ta^{5+} looks as the most suitable supposition for the Fe2 center. In this case there are lithium nuclei in the first three shells of the nearest surrounding, and the distances from tantalum site to these nuclei are about 3–3.4 Å (Figs. 7 and 8). The distances are smaller than the distance between lithium site and lithium shells (3.8 Å or more) in the case of $Fe^{3+}{}_{Li}$ center.

Hyperfine interaction decreases usually with the distance R between paramagnetic ion and lattice nucleus. For instance, the dipole-dipole part of the interaction decreases as $1/R^3$. Therefore, hyperfine splittings for $Fe^{3+}{}_{Ta}$ should be approximately two times larger than for $Fe^{3+}{}_{Li}$. This agrees with the observed splittings for Fe2 and Fe1. The ratio $b_2{}^0(\mathrm{Fe2})/b_2{}^0(\mathrm{Fe1}) < 1$ also supports the $Fe^{3+}{}_{Ta}$ model for the Fe2 centers, since $Fe^{3+}{}_{Ta}$ has six monovalent lithium ions behind the nearest oxygen surrounding, whereas $Fe^{3+}{}_{Li}$ has six pentavalent tantalum ions. It should be mentioned that in $LiNbO_3$ crystals the $Fe^{3+}{}_{Nb}$ centers have also smaller values of the axial crystal filed than the $Fe^{3+}{}_{Li}$ ones.

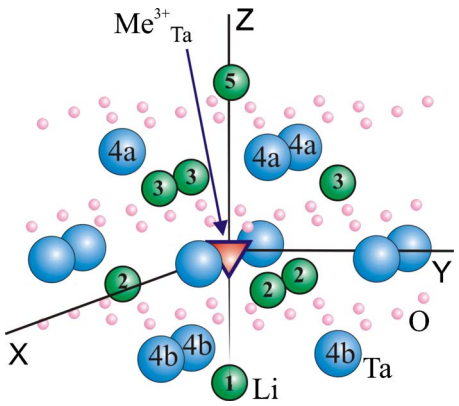

FIG. 8. (Color online) Schematic representation of surroundings of an ion substituting for Ta in $LiTaO_3$.

Finally, the supposition allows understanding the observed increase of I_2/I_1 ratio with the rise of total concentration of iron in the samples. The VTE treated samples have significantly reduced concentration of intrinsic defects, which can serve as charge compensators for a limited amount of $Fe^{3+}{}_{Li}$ centers. If the iron concentration exceeds the intrinsic defects concentration, another mechanism of the charge compensation becomes more preferable, namely, self-compensation of $Fe^{3+}{}_{Li}$ and $Fe^{3+}{}_{Ta}$ centers. Farther increase of the total iron concentration leads to the rise of the Fe2 centers concentration, and I_2 approaches I_1. Just this picture was observed in our experiments.

IV. CONCLUSION

We have found the second axial Fe2 center in VTE treated lithium tantalate crystals. The center has smaller axial crystal field parameters than the previously observed Fe1 center. It is very difficult to prove that the Fe2 centers do not exist in congruent crystals due to very large width of the EPR lines. However, we can state that the ratio of I_2/I_1 is less than 0.1 or even less.

To our opinion, there are two critical parameters, which stimulate the appearance of the Fe2: the deviation of the crystal composition from stoichiometry $\delta=([\mathrm{Li}]-[\mathrm{Ta}])/([\mathrm{Li}]+[\mathrm{Ta}])$ and the total concentration of iron ions in the sample [Fe]. If $\delta \gg [\mathrm{Fe}]$ the Fe1 centers are dominating. If $\delta \ll [\mathrm{Fe}]$ the Fe2 centers are dominating. The presence of the Fe2 centers in the samples with $[\mathrm{Fe}] \approx 6.7 \times 10^{19}$ cm^{-3} is a strong evidence that thermal and temporal regimes used at the VTE treatment turned the congruent LT samples into samples with practically stoichiometric composition.

Our ENDOR data support the $Fe^{3+}{}_{Ta}$ model for the Fe2 centers. The appearance of the $Fe^{3+}{}_{Ta}$ centers after the VTE treatment of congruent samples, in which only the $Fe^{3+}{}_{Li}$ were present, means that all ions—Li, Ta, and Fe—change their lattice sites at this treatment.

Some questions are still not answered. It is not clear why two additional axial centers appear in stoichiometric LN and only one additional center appears in sLT. The sLT samples were already studied by different techniques including the EPR. However, the $Me^{3+}{}_{Ta}$ centers were not registered in the samples, which were called "stoichiometric." We hope that further inquiry of undoped or doped LT samples of different compositions should shed light on these problems.

ACKNOWLEDGMENTS

Authors are grateful to Dr. V. Bratus for testing measurements of low doped samples. The work was supported by the NSF (Grant Nos. 0307267, 0436039, and 0514463) and by the Montana Board of Research and Commercialization Technology (Grant No. 405-613).

[1] M. G. Clark, F. J. DiSalvo, A. M. Glass, and G. E. Peterson, J. Chem. Phys. **59**, 6209 (1973).
[2] E. Kraetzig and R. Orlowski, Appl. Phys. **15**, 133 (1978).
[3] A. Räuber, in *Current Topics in Material Science*, edited by E. Kaldis (North-Holland, Amsterdam, 1978), Vol. 1, pp. 481–600.
[4] O. F. Schirmer, O. Thiemann, and M. Woehlecke, J. Phys. Chem. Solids **52**, 185 (1991).
[5] J. Imbrock, D. Kip, and E. Kratzig, Opt. Lett. **24**, 1302 (1999).

[6]R. Ryf, G. Montemezzani, P. Gunter, Y. Furukawa, and K. Kitamura, Appl. Phys. B: Lasers Opt. **72**, 737 (2001).
[7]H. Soethe, L. G. Rowan, and J.-M Spaeth, J. Phys.: Condens. Matter **1**, 3591 (1989).
[8]V. A. Vazhenin, V. B. Guseva, M. Y. Artyomov, R. K. Route, M. M. Fejer, and R. L. Byer, J. Phys.: Condens. Matter **15**, 275 (2003).
[9]M. Loyo-Menoyo, D. J. Keeble, Y. Furukawa, and K. Kitamura, J. Phys.: Condens. Matter **16**, 9047 (2004).
[10]G. Malovichko, OSA Trends Opt. Photonics Ser. **27**, 59 (1999).
[11]P. F. Bordui, R. G. Norwood, C. D. Bird, and G. D. Calvert, J. Cryst. Growth **113**, 61 (1991).
[12]D. H. Jundt, M. M. Fejer, and R. L. Byer, IEEE J. Quantum Electron. **26**, 135 (1990).
[13]N. Iyi, K. Kitamura, F. Izumi, J. K. Yamamoto, T. Hayasgi, H. Asano, and S. Kimura, J. Solid State Chem. **101**, 340 (1992).
[14]K. Kitamura, Y. Furukawa, and N. Iyi, Ferroelectrics **202**, 21 (1997).
[15]G. I. Malovichko, V. G. Grachev, L. P. Yurchenko, V. Ya. Proshko, E. P. Kokanyan, and V. T. Gabrielyan, Phys. Status Solidi A **133**, K29 (1992).
[16]G. I. Malovichko *et al.*, Appl. Phys. A: Solids Surf. **A56**, 103 (1993).
[17]A. Kling, J. G. Marques, J. G. Correia, M. F. da Silva, E. Dieguez, F. Agullo-Lopez, and J. C. Soares, Nucl. Instrum. Methods Phys. Res. B **113**, 293 (1996).
[18]V. Bermudez, P. S. Dutta, M. D. Serrano, and E. Dieguez, J. Phys.: Condens. Matter **9**, 6097 (1997).
[19]K. Polgar, A. Peter, L. Kovacs, G. Corradi, and Zs. Szaller, J. Cryst. Growth **177**, 211 (1997).
[20]P. Bernasconi, G. Montemezzani, P. Gunter, Y. Furukawa, and K. Kitamura, Ferroelectrics **223**, 373 (1999)
[21]V. Ya. Shur, E. V. Nikolaeva, E. I. Shishkin, V. L. Kozhevnikov, A. P. Chernykh, K. Terabe, and K. Kitamura, Appl. Phys. Lett. **79**, 3146 (2001).
[22]M. Katz, R. K. Route, D. S. Hum, K. R. Parameswaran, G. D. Miller, and M. M. Fejer, Opt. Lett. **29**, 1775 (2004).
[23]L. Tian, V. Gopalan, L. Galambos, Appl. Phys. Lett. **85**, 4445 (2004).
[24]Y. Furukawa, K. Kitamura, E. Suzuki, and K. Niwa, J. Cryst. Growth **197**, 889 (1999).
[25]V. T. Kalinnikov, O. G. Gromov, G. B. Kunshina, A. P. Kuz'min, E. P. Lokshin, and V. I. Ivanenko, Inorg. Mater. **40**, 411 (2004).
[26]G. I. Malovichko, V. G. Grachev, O. F. Schirmer, and B. Faust, J. Phys.: Condens. Matter **5**, 3971 (1993).
[27]G. Malovichko, V. Grachev, E. Kokanyan, and O. Schirmer, Phys. Rev. B **59**, 9113 (1999).
[28]V. Grachev, G. Malovichko, and E. Kokanyan, Ferroelectrics **258**, 131 (2001).
[29]J. Imbrock, C. Baeumer, H. Hesse, D. Kip, and E. Kraetzig, Appl. Phys. B: Lasers Opt. **78**, 615 (2004).